THE SEARCH FOR PROTON DECAY*

R. Bionta, G. Blewitt, C.B. Bratton, D. Casper, B. G. Cortez, S. Errede, G.W. Foster, W. Gajewski, K.S. Ganezer, M. Goldhaber, T.J. Haines, T.W. Jones, D. Kielczewka, W.R.Kropp, J.G. Learned, E. Lehmann, J.M. LoSecco, H.S. Park, F. Reines, J. Schultz, S. Seidel, E. Shumard, D. Sinclair, H.W. Sobel, J.L. Stone, L.R. Sulak, R. Svoboda, J.C. van der Velde, and C. Wuest

The University of California at Irvine, Irvine, California 92717, and The University of Michigan, Ann Arbor, Michigan 48109, and Brookhaven National Laboratory, Upton, New York 11973, and California Institute of Technology, Pasadena, California 91125, and Cleveland State University, Cleveland, Ohio 44115, and The University of Hawaii, Honolulu, Hawaii 96822, and University College, London WC1E 6BT, United Kingdom

ABSTRACT

Following a very brief description of the theoretical developments which motivated the search for proton decay, I shall describe one of these experiments (the IMB experiment) in some detail. Then I shall compare recent results from that experiment with those from other detectors.

WHY SEARCH FOR PROTON DECAY?

Protons and neutrons are the building blocks of the chemical elements but they are not truly elementary particles, they are composite structures. They are composed of quarks. The proton consists of two u quarks and one d quark, while the neutron is two d quarks and one u quark. Though u quarks may change into d quarks and vice versa, in all the known elementary processes, the total number of quarks always remains the same. For example in ordinary β-decay

$$\underset{\text{neutron}}{(u,\ d,\ d)} \rightarrow \underset{\text{proton}}{(u,\ u,\ d)} + e^- + \bar{\nu}.$$

There are the same number of quarks before and after the transition. One of the quarks simply changed its flavor.

Starting in 1974, Grand Unified Theories (GUTS) were developed. Among other things these theories unified the electromagnetic and

*Talk presented by D. Sinclair at the Conference on the Intersections between Particle and Nuclear Physics, Steamboat Springs, 1984

0094-243X/84/1230321-16 $3.00

nuclear forces and provided a framework for understanding the elementary processes by which matter (protons and electrons) was created at the birth of the Universe. It is a feature of these theories that quarks can turn into leptons - but with very low probability - hence it follows that nucleons are unstable. The simplest version of the GUTS, introduced by Georgi and Glashow[1], is known as minimal SU(5). It predicts as follows:

mainly $p \rightarrow e^+ + \pi^\circ$
$n \rightarrow e^+ + \pi^-$

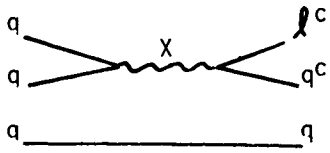

with a lifetime of approximately 10^{30} years. The lifetime is so long because the mass of the intermediate X boson is enormous, approximately 10^{15} GeV.

The crucial test of this theory is therefore to search for proton decay at the level of 10^{30} years. This is an incredibly long time as demonstrated by comparison with other "long times" familiar to physicist shown in the table below.

Table I Some examples of "long times"

Half life of ^{238}U	4.5×10^9 yr.
Age of earth	4.6×10^9 yr.
Time since "Big Bang"	$\sim 1.5 \times 10^{10}$ yr.
Half life of ^{238}U for spont. fission	$\sim 10^{16}$ yr.
Half life of ^{130}Te for double β-decay	1.4×10^{21} yr.

THE IMB EXPERIMENT

Descriptions of the IMB detector already exist in published letters[2,3,4] and the theses of several students[5,6,7,8]. It is a ring-imaging water Cherenkov detector located at a depth of 1570 meters of water equivalent in the Morton-Thiokol salt mine east of Cleveland, Ohio. It consists of a large rectangular volume of purified water (17x18x23 m^3) viewed from its six faces by 2048 photomultiplier tubes (PMT), each of 12.5 cm diameter, located on a rectangular grid of ~ 1 m spacing. The total volume of the detector is 8000 m^3 (2.0×10^{33} nucleons). Relativistic charged particles from nucleon decays or entering cosmic rays are detected by their Cherenkov light impinging on the PMT's. The readout electronics independently records for each tube the time of arrival (T1) and the pulse height due to Cherenkov light at that tube. The PMT's are operated at sufficiently high gain to detect with high probability ($\gtrsim$ 60%) the emission of single photo-electrons from the

photo-cathode. The light level of Cherenkov radiation is extremely low. Just how low is demonstrated by the following examples.

Table II Some examples of "low illumination"

Moonlight	10^{16} photons/m^2/s
Starlight	10^{13} photons/m^2/s
A candle 100 miles away	10^6 photons/m^2/s
Photoflash on the moon	1000 photons/m^2 on earth
Cherenkov light from charged particle at 10 m distance in water	300 photons/m^2

The T1 time scale has a least count of 1 ns, compatible with a time resolution of 5.5 ns HWHM for a typical PMT, and the T1 clock runs for 500 ns. Following a trigger on the T1 time scale, the electronics activates, for each PMT, a second time scale (T2) for an additional 7.5 μs, enabling the detection of $\mu^+ \to e^+ \nu\bar{\nu}$ decays with an efficiency ~ 65%, and μ^- decays at ~ 55%.

CALIBRATION OF THE IMB DETECTOR

The response of the detector to cosmic ray muons, neutrino interactions and various modes of nucleon decay is simulated by a computer program which uses Monte Carlo techniques. Many of the program's parameters are determined from the physics of the processes. Examples include:

1. Cherenkov light production.
2. Electromagnetic interactions of muons and electrons, including delta-ray production[5].
3. Cosmic ray muon polarization and charge ratio[8].
4. Muon absorption and depolarization in water[8].
5. dE/dx losses of charged particles in water.
6. Pion and kaon nuclear cross sections[3,8].

Other parameters are obtained directly from measurements. These include:

1. Absorption of light in the water. This is measured by a moveable light source consisting of a diffusing ball connected to a N_2 laser through an optical fiber.

2. The response of each PMT - that is pulse size versus light intensity. This is measured using a N_2 laser connected through an optical fiber to a diffusing ball located at the center of the detector. The intensity of the light pulses is varied by inserting a series of neutral filters into the laser beam.
3. The time response of each PMT, measured as in item 2 above.

Lastly there are some parameters which can be determined only by comparing the simulation program with the detector response to certain physical process and "tuning" the simulation program accordingly. These are:

1. Light scattering probability. This is determined using the light scattered outside the Cherenkov cone of cosmic ray muons.

2. Average PMT firing efficiency. That is the probability that a photo electron will be emitted by a photon striking the photo-cathode times the probability that it will produce a pulse above the discriminator threshold. The answer is ~ 0.16 though individual tubes vary by ± 20% about this mean.

3. The relation between the total light yield of an event, determined by adding the pulses of the PMT's which fire, and the Cherenkov equivalent energy (E_C) of the event.

A selected set of vertical muons passing through the center of the detector are used to determine the parameters of items 2. and 3. The quantity "Cherenkov equivalent energy" may require some explanation. Charged particles produce light at velocities above 0.75 c in water, and hence $\mu^{\pm}$, $\pi^{\pm}$ and $K^{\pm}$ are visible above total energy thresholds of 160, 215 and 750 MeV respectively. By contrast $e^{\pm}$, γ and π°'s produce electromagnetic showers in which essentially all of the energy is deposited by electrons or positrons with velocities above the Cherenkov threshold. There is, therefore, a factor which converts total light yield to total energy for nucleon decay modes whose secondaries are $e^{\pm}$, π°'s or γ's. When the secondaries include $\mu^{\pm}$, $\pi^{\pm}$ etc. the energy obtained by multiplying total light yield by this factor is the Cherenkov equivalent energy (E_C) and it is less than the total energy. Pulse size is measured in units of the mean pulse size for single photo electrons (SPE). The conversion factor is measured to be approximately 4 MeV per SPE with an uncertainty of ±15%.

DATA REDUCTION

Descriptions of data reduction procedures can be found in the theses[5,6,7,8]. In this talk I shall provide only a brief outline. The goal of the analysis is to identify events with vertices inside the fiducial volume - "contained events". Contained events must be either neutrino interactions or new physics - nucleon decay. Two independent analysis chains are used to cross-check the results.

In the search for nucleon decay we first require that the number of illuminated PMT's (NPT) lie in the range $40 \leq NPT \leq 300$. The mean NPT for decay modes with maximum light yields, e.g. $p \rightarrow e^+\gamma$, is ~175, so that the efficiency of this requirement is ~100% for such modes. For decay modes with a low Cherenkov light yield, this efficiency can be low, e.g. $p \rightarrow \mu^+\rho^\circ$ has an efficiency of ~30%. The next step is to use the timing and the topology of the PMT's that fired to determine the event vertex. The mean error of the vertex determination varies between 0.5 and 1.0 m for various nucleon decay modes, as measured by computer simulation of these modes. Also measured in this way is the efficiency of the event fitting procedures which is > 80% for both nucleon decays and neutrino interactions. Starting with 4.7×10^7 triggers for 204 days of live time, the procedures outlined above reduced this number to ~300 events with vertices inside the fiducial volume. One additional cut, described in Figure 1, plus some scanning on the color graphics system, further reduced the number to a final sample of 169 contained events. The vertex of 24 of these events was adjusted by hand using the color graphics system.

PROPERTIES OF CONTAINED EVENTS

The important question to ask about the contained events is this: Are their characteristics what one would expect from neutrino interactions or is there evidence of some new phenomena such as nucleon decay? To answer this question we look at various properties of the contained events. First we look at the rate. We find 0.8 events per day. Using the atmospheric neutrino flux computed by T. Gaisser[9] we estimate 0.9 events per day. To obtain this estimate we got topologies and track energies from bubble chamber neutrino data as described in reference 6, and passed the simulated events through the same analysis chain as the data.

Next we look at the energy distribution of the contained events (actually the quantity E_c, as defined in the section on calibration) and their momentum imbalance. As a measure of momentum imbalance we define a parameter A ("Anisotropy") which is the magnitude of the vector sum of unit vectors from the fit vertex to each lit PMT, normalized by the total number of lit PMT's. A is ~0.7 (the cosine of the Cherenkov angle) for the events with a single visible track and ≤ 0.3 for events with two visible tracks and a wide opening angle. A scatter plot of E_c vs. A for the 169 contained events from 204 live days is given in Figure 2(a). This should be compared with Figure 2(b) which is E_c vs. A for a simulation of 204 days of atmospheric neutrino interactions obtained by using bubble chamber data to provide energies, and topologies. We weighted the events to correct for the difference between the energy spectrum of the bubble chamber events and atmospheric neutrino interactions. Events with 0, 1, >2 identified muon decays are indicated by '•', 'X' and '*'

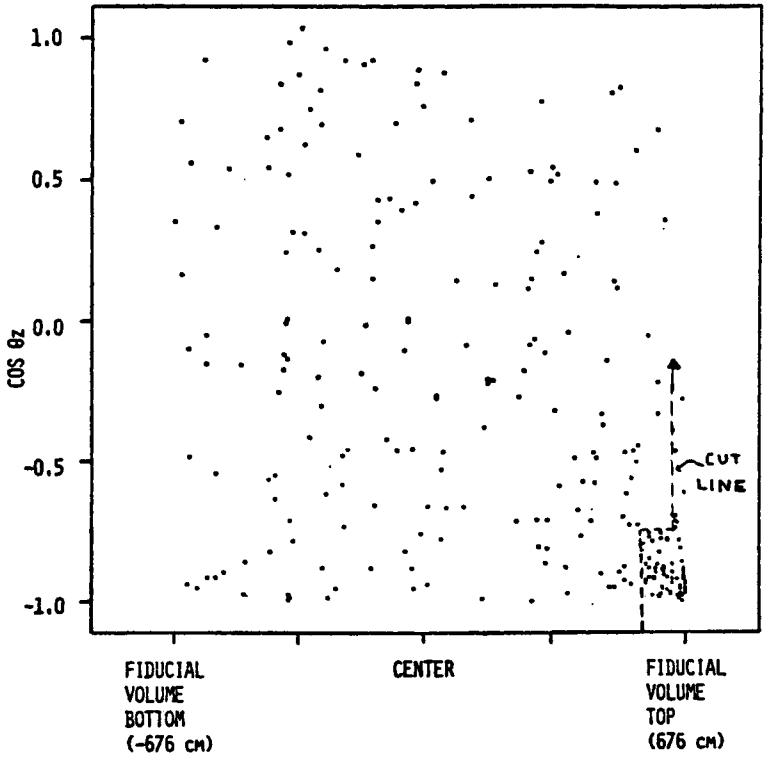

Figure 1. Fit z vertex positions vs. fit z direction cosines of events fit inside the fiducial volume of the IMB detector. Note the excess of events in the lower right corner (downward-going and entering in the top). The cuts made to eliminate this background are indicated by the dashed lines. The cuts reduce the fiducial volume by 2.5%. the figure is from the thesis of E. Shumard (Ref. 8).

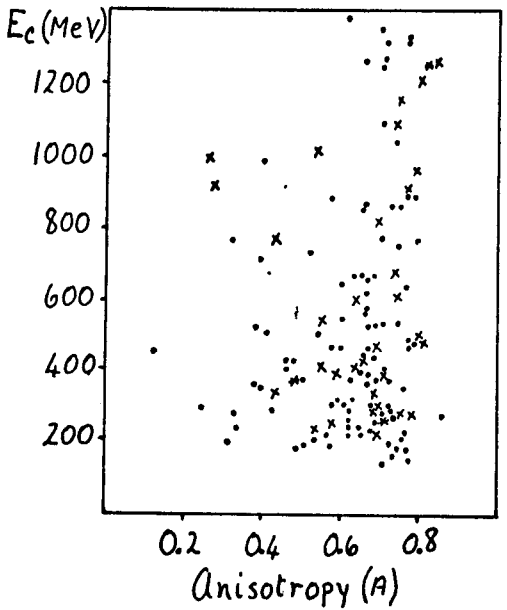

Figure 2(a).

E_c vs. A for the 169 contained events from 204 live days of data from the IMB detector. Events with 0,1, and >2 identified $\mu \rightarrow e$ decays are indicated by '•', 'X' and '*' respectively.

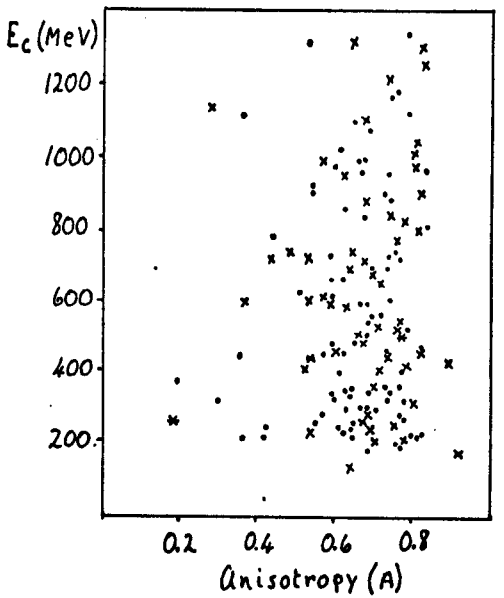

Figure 2(b).

E_c vs. A for a simulation of 204 days of atmospheric neutrino interactions. The number of background events for each mode was determined from a 6.5 year ν simulation.

respectively. Agreement between the two scatter-plots is good, and certainly within our estimate of the errors. Uncertainties in the calculation of neutrino flux are ±30%. However other considerations such as possible scanning biases in the bubble chamber data, nuclear effects from pion absorption, ambiguity in the identification of π^+ and p, lead us to assign considerably higher errors (+100%, -50%) to sparsely populated regions of the scatterplot.

IMB LIMITS ON SPECIFIC MODES OF NUCLEON DECAY

Search for the signal corresponding to a specific nucleon decay mode proceeds by selecting a region of the scatterplot appropriate for the mode under consideration and looking for events in that region. In addition we require the presence or absence of an observed muon decay as appropriate. For the four decay modes which should possess a clear two-body decay signature, viz. $p \to e^+\gamma$, $p \to \mu^+\gamma$, $p \to e^+\pi^\circ$, $p \to \mu^+\pi^\circ$ we require that two clearly defined tracks with opening angles > 140° be recognized on the graphics display, and include for these modes an efficiency factor evaluated by hand scanning of simulated events. As an example, Figure 3 shows a scatterplot of simulated nucleon decays by the mode $p \to e^+\pi^\circ$. The solid lines define the region of the scatterplot in which a search is made for decays of this type. According to the simulation it should contain 70% of the events. Nuclear interaction of the π° in the oxygen nucleus is the main reason 30% of the events lie outside the box.

Limits on various modes of nucleon decay obtained by the method outlined above are listed in Tables III, IV, and V. The overall detection efficiencies (normalized to the fiducial mass) are presented in two forms: a) with all nuclear effects included (we use this efficiency to obtain our lifetime limits), and b) with only Fermi motion and $\pi^\pm$ interactions in the surrounding water taken into account. This is useful to relate our efficiencies to those of other experiments in a way which does not depend on the nuclear model. The lifetime limits quoted are at the 90% confidence level for 204 live days and do not include background subtraction. Because of the large errors associated with the background estimate we felt a background subtraction was not justified. The number of contained events passing all requirements for each mode are listed in the third from last column. Since many events are candidates for more than one mode, there are many fewer candidate events (in total) than the sum of the entries in this column. Actually there are only six candidate events for all the non-ν modes (Tables III and IV). These six events are listed in Table VI.

We have investigated the effects on lifetime limits arising from possible systematic errors on E_c (±15%) and A (±.05). These errors produce changes in the 90% C.L. lifetime limits which are less than a factor of two in all cases.

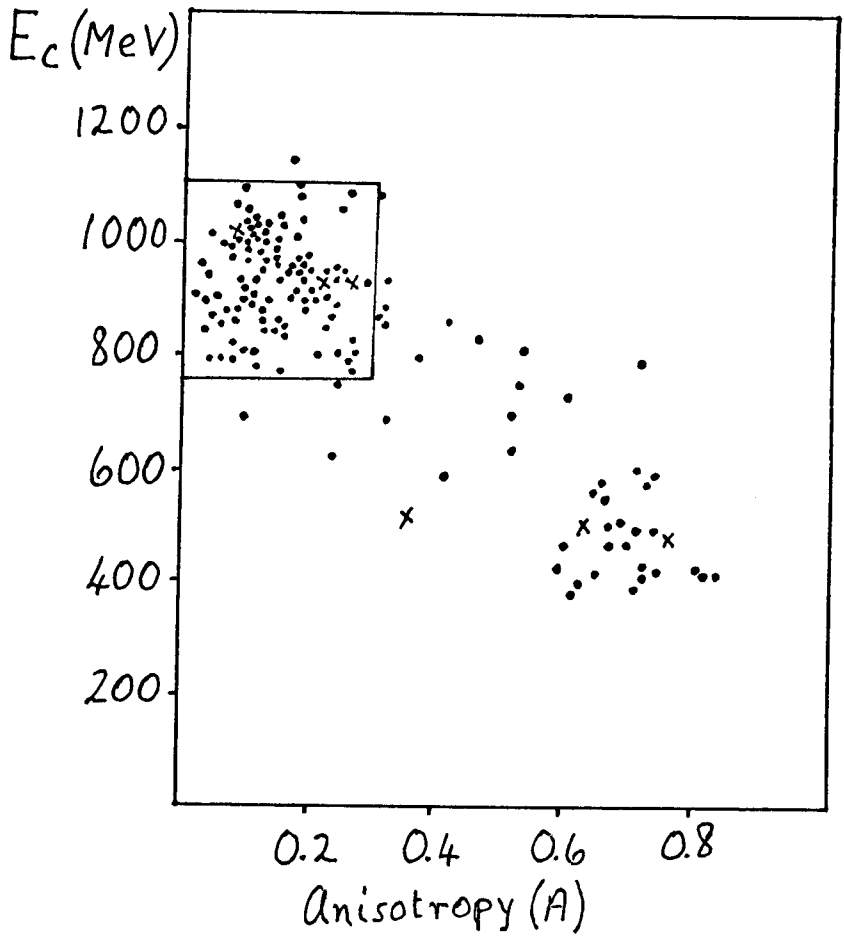

Figure 3. E_c vs. A for a sample of simulated decays $p \to e^+\pi^\circ$; $\pi^\circ \to \gamma\gamma$. The square box indicates the region in which candidates are accepted for this mode. Nuclear interactions of the π° are the main reason 30% of the events lie outside the box.

Table III Current Limits from IMB - Two body modes

Mode	Requirements E_C (MeV)	A	#μ	Effic. with N.C.	Effic. without N.C.	# of Cand. Obs.	# of Bkgrd. Est.	Limit τ/β $\times 10^{31}$yr
$p \to e^+\pi^\circ$	750-1100	<.3	0	0.54	0.75	0	0.2	15.
$p \to \mu^+\pi^\circ$	550-850	.1-.4	1	0.38	0.41	0	0.6	10.
$p \to e^+\gamma$	750-1100	<.4	0	0.74	0.74	0	0.1	20.
$p \to \mu^+\gamma$	550-800	<.5	1	0.47	0.47	0	0.4	13.
$n \to e^+\pi^-$	500-950	.15-.5	0	0.33	0.49	4	3	2.1
$n \to \mu^+\pi^-$	200-700	.1-.5	1	0.42	0.42	1	4	5.0
$n \to e^-\pi^+$	400-950	.1-.5	0,1	0.24	0.31	2	4	4.1
$n \to \mu^-\pi^+$	200-550	.1-.5	1,2	0.30	0.48	2	3	2.9

Notes:

a) Limits based on 204 live days, 90% C.L., and no background subtraction.
b) The first 4 modes have additional requirement of two clear tracks with opening angle > 140°.

Table IV Current Limits from IMB - Pseudo 3-body Modes

Mode	Requirements E_c (MeV)	A	#μ	Effic. with N.C.	Effic. without N.C.	# of Cand. Obs.	# of Bkgrd. Est.	Limit τ/β $\times 10^{31}$ yr
$p \to e^+ \eta^\circ$	750-1100	<.3	0	0.41	0.41	0	0.2	11.
$p \to \mu^+ \eta^\circ$	550-850	<.4	1	0.31	0.31	0	0.6	9.
$p \to e^+ \rho^\circ$	300-600	.15-.5	1	0.12	0.16	1	3	1.9
$p \to \mu^+ \rho^\circ$	175-400	.15-.5	1,2	0.16	0.16	2	2	1.9
$p \to e^+ \omega^\circ$	300-600	.1-.5	1	0.12	0.23	1	3	2.0
$p \to e^+ K^\circ$	†	†	†	0.31	0.32	1	3	6.
$p \to \mu^+ K^\circ$	†	†	†	0.35	0.36	2	5	6.
$p \to e^+ e^+ e^-$	750-1100	<.3	0	0.93	0.93	0	0.2	25.
$p \to \mu^+ \mu^+ \mu^-$	200-425	<.5	2,3	0.57	0.57	1	0.2	9.
$n \to e^+ \rho^-$	500-850	.1-.5	0	0.38	0.56	4	3	2.4
$n \to \mu^+ \rho^-$	250-625	.1-.5	1	0.22	0.41	1	4	2.8
$n \to e^- \rho^+$	500-850	.1-.4	1	0.12	0.33	0	1	2.6
$n \to \mu^- \rho^+$	225-600	.1-.5	1,2	0.25	0.43	2	4	2.4

Notes:

a) Limits based on 204 live days, 90% C.L. and no background subtraction.
b) For $p \to 3e$ and $p \to 3\mu$, flat phase space was assumed.
c) The efficiencies include meson branching ratios as well as detection efficiencies.
d) Some events are candidates for more than one mode.

Table V Current Limits from IMB - Modes with ν

Mode	Requirements E_C (MeV)	A	#μ	Effic. with N.C.	Effic. without N.C.	# of Cand. Obs.	# of Bkgrd. Est.	Limit τ/β $\times 10^{31}$yr
$p \to \nu K^+$	150-375	.3-.65	1	0.11	0.11	3	6	1.
$p \to \nu K^{*+}$	250-500	.3-.6	1	0.09	0.18	4	4	0.7
$n \to \nu \pi^\circ$	325-625	.5-.8	0	0.56	0.88	30	23	0.7
$n \to \nu \eta^\circ$	475-800	.15-.5	0	0.54	0.54	4	2	3.4
$n \to \nu \gamma$	325-600	.6-.8	0	0.76	0.76	26	18	1.1
$n \to \nu \omega^\circ$	200-425	.3-.65	1	0.16	0.24	6	7	0.8
$n \to \nu K^\circ$	450-750	.2-.5	0	0.11	0.11	3	2	0.8
$n \to \nu K^{+\circ}$	200-700	.15-.5	1	0.06	0.12	1	4	0.7
$n \to e^+e^-\nu$	500-850	<.5	0	0.41	0.41	4	3	2.6
$n \to \mu^+\mu^-\nu$	150-375	.2-.65	1,2	0.30	0.30	4	7	2.0

Notes:

a) Limits based on 204 live days, 90% C.L., and no background subtraction.

Table VI Candidates for non-ν Modes from IMB

IMB Event No.	Energy E_c(MeV)	Anisotropy A	#μ	Decay Modes
299-72044	770	0.32	0	$e^+\pi^-$, $e^+\rho^-$, $e^-\pi^+$
510-54208	720	0.39	0	$e^+\pi^-$, $e^+\rho^-$, $e^-\pi^+$
588-8320	370	0.49	2	$\mu^+\rho^\circ$, $\mu^+\omega^\circ$, μ^+K°, $\mu^+\mu^+\mu^-$, $\mu^-\pi^+$, $\mu^-\rho$
656-11673	530	0.38	0	$e^+\pi^-$, $e^+\rho^-$
663-1770	500	0.41	0	$e^+\pi^-$, $e^+\rho^-$
747-44203	340	0.43	1	$e+\rho^\circ$, $\mu^+\rho^\circ$, $e^+\omega^\circ$, $\mu^+\omega^\circ$, e^+K°, μ^+K°, $\mu^+\pi^-$, $\mu^+\rho^-$, $\mu^-\pi^+$, μ^-e

RESULTS FROM OTHER DETECTORS

Significant results have been reported from four other detectors. These are:

The Kolar Gold Field Experiment - Tata, Osaka, Tokyo. This detector is iron plates interleaved with proportional chambers. It has a total mass of 140 ton. 26 contained events have been detected in 1000 days of live time. Four of these have topologies which exhibit momentum balance.

The Mont Blanc Detector - Frascati, Milan, Torino, CERN. Iron plates interleaved with streamer chambers. This detector has a total mass of 150 tons. 10 contained events have been reported from 317 live days. One event is said to be a good candidate for $p\to K^\circ\mu$, $K^*\mu$ or 3μ, though it could be a neutrino interaction. Neutrino events "expected in this topology are less than 0.09". (See reference 10).

The HPW Experiment - Harvard, Purdue, Wisconsin. This detector is located in the Silver King Mine at Park City, Utah. It is a water Cherenkov detector with a total mass of 700 tons. At the Washington APS meeting in April '84, results were reported on 315 days of operation. Neutrino events observed were said to be consistent with the expected rate. Two events were observed with double μ-decay and based on this, limits were derived for several modes of nucleon decay.

The Kamioka Experiment - This detector is the work of a Japanese collaboration consisting of KEK, Tokyo, Niigata and Tsukuba universities. It is a ring-imaging water Cherenkov detector with a total mass of 3000 ton and a fiducial mass of 1000 ton. It contains 1000 20" diameter PMT's on a 1 m grid, viewing a cylindrical volume 14 m in diameter and 14 m high. Although it is smaller than the IMB detector (by a factor of 3) it has considerably more sensitivity to light (~12 times more) so it is more able to distinguish individual tracks when the Cherenkov rings overlap.

The results shown here are preliminary. They were presented at the ICOBAN meeting in January '84 and are for 118 live days. In that time they found 57 contained events in a fiducial volume of 1000 tons. In Table VII these events have been classified according to the number of rings that can be resolved and whether or not there is a μ decay associated with the event. The characteristics of events expected from ν-interactions are also shown. Table VIII gives 90% C.L. limits on the lifetime of various modes of proton decay.

Table VII Kamioka Detector. KEK, Tokyo, Niigata, Tsukuba.

3000 ton water Cherenkov
1000 ton fiducial volume
20" DIA. PMT's 1 m spacing
(12 times light sensitivity of IMB)

Preliminary results reported for 118 days (324 ton yr.)

Number of Rings	Data		Expected from ν	
	Total	With μ decay	Total	With μ decay
1	40	8	44	18
2	8	1	4.5	1.5
3	5	2.5	3.0	1.6
4	2	2	2.0	0.6
5	2	1	0	0
Total	57	14.5	52.5	21.7

Table VIII KAMIOKA - Preliminary results for lifetime limits

90% C.L. - 324 ton-yr (~ 1/6 of IMB)

Decay Mode	Detection Efficiency	Expected ν Bkgrd.	No. Cand.	Limit τ/β (10^{31} yr.)
$p \to e^+\pi^\circ$	0.55	0	0	2.6
$e^+\eta^\circ$	0.38	0	0	1.8
$e^+\omega^\circ$	0.6	2.1	1	1.7
$e^+\rho^\circ$	0.45	1.8	0	2.1
$e^+K^\circ(2\pi^\circ)$	0.16	0	0	1.8
$(\pi^+\pi^-)$	0.23	0.2	0	1.8
$e^+K^{*\circ}$	0.37	0.1	0	1.8
$p \to \mu^+\pi^\circ$	0.48	0.1	0	2.3
$\mu^+\eta(2\gamma)$	0.27	0	1	0.8
$\mu^+\omega^\circ$	0.22	0.5	0	1.0
$\mu^+\rho^\circ$	0.35	0.1	0	1.7
$\mu^+K^\circ(2\pi^\circ)$	0.11	0	1	0.8
$(\pi^+\pi^-)$	0.16	0	0	
$p \to \nu\pi^+$	0.22	5.5	5	0.3
$\bar{\nu}\rho^+$	0.5	1.2	2	1.0
$\nu K^+(\mu^+\nu)$	0.28	0.8	2	0.7
$(\pi^+\pi^\circ)$	0.16	0.2	1	
νK^{*+}	0.62	1.7	4	0.8

CONCLUSION

In conclusion, proton decay into modes with a clear two body signature, such as $p \to e^+\pi^\circ$ or $p \to e^+\gamma$ are excluded to the level of about 1-2 x 10^{32} yr. Modes which produce more complicated topologies are ambiguous with neutrino events and lifetime limits for these modes are a few x 10^{31} years.

REFERENCES

1. H. Georgi and S.L. Glashow, Phys. Rev. Lett. 32, 438 (1974), For reveiw of Grand Unified Theories, see P. Langacker, Phys. Rev. 72, 185 (1981).
2. R. Bionta et al., Phys. Rev. Lett. 51, 27 (1983).
3. T. Jones et al., Phys. Rev. Lett. 52, 720 (1984).
4. B. Cortez et al., Phys. Rev. Lett. 52, 1092 (1984).
5. G.W. Foster, Ph.D thesis, Harvard University (1983).
6. B. Cortez, Ph.D thesis, Harvard University (1983).
7. C. Wuest, Ph.D thesis, University of California at Irvine (1984).
8. E. Shumard, Ph.D thesis, University of Michigan (1984).
9. T. Gaisser and T. Stanev, Phys. Rev. D. 27
10. Proceedings of the International Symposium on Lepton and Photon Interactions at High Energies, Cornell University, 1983.